Environmental Science & Technology

pubs.acs.org/est

Article

Mechanistic Implications of the Varying Susceptibility of PAHs to Pyro-Catalytic Treatment as a Function of Their Ionization Potential and Hydrophobicity

Sara B. Denison, Peixuan Jin, Kyriacos Zygourakis, Thomas P. Senftle,* and Pedro J. J. Alvarez*

Cite This: *Environ. Sci. Technol.* 2024, 58, 13521−13528

Read Online

ACCESS | Metrics & More | Article Recommendations | Supporting Information

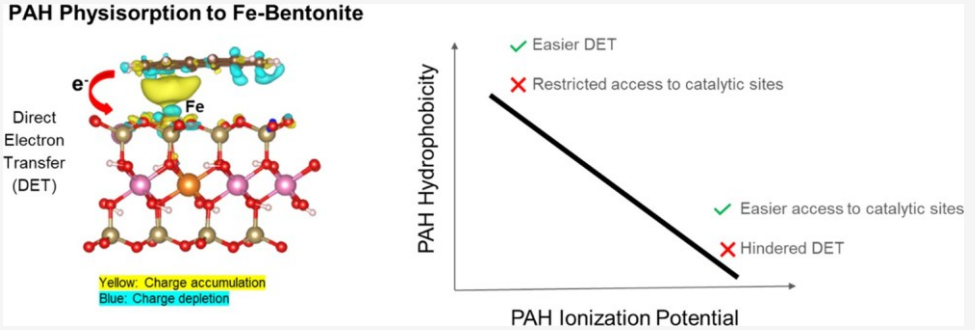

ABSTRACT: Transition metal catalysts in soil constituents (e.g., clays) can significantly decrease the pyrolytic treatment temperature and energy requirements for efficient removal of polycyclic aromatic hydrocarbons (PAHs) and, thus, lead to more sustainable remediation of contaminated soils. However, the catalytic mechanism and its rate-limiting steps are not fully understood. Here, we show that PAHs with lower ionization potential (IP) are more easily removed by pyro-catalytic treatment when deposited onto Fe-enriched bentonite (1.8% wt. ion-exchanged content). We used four PAHs with decreasing IP: naphthalene > pyrene > benz(a)anthracene > benzo(g,h,i)perylene. Density functional theory (DFT) calculations showed that lower IP results in stronger PAH adsorption to Fe(III) sites and easier transfer of π-bond electrons from the aromatic ring to Fe(III) at the onset of pyrolysis. We postulate that the formation of aromatic radicals via this direct electron transfer (DET) mechanism is the initiation step of a cascade of aromatic polymerization reactions that eventually convert PAHs to a non-toxic and fertility-preserving char, as we demonstrated earlier. However, IP is inversely correlated with PAH hydrophobicity (log K_{ow}), which may limit access to the Fe(III) catalytic sites (and thus DET) if it increases PAH sorption to soil OM. Thus, ensuring adequate contact between sorbed PAHs and the catalytic reaction centers represents an engineering challenge to achieve faster remediation with a lower carbon footprint via pyro-catalytic treatment.

KEYWORDS: *pyrolysis, catalysis, soil remediation, PAHs, direct electron transfer, clays*

INTRODUCTION

Polycyclic aromatic hydrocarbons (PAHs) consist of over 100 compounds containing multiple fused benzene rings originating from natural and anthropogenic sources.[1] The U.S. Environmental Protection Agency (EPA) currently regulates 16 potentially mutagenic and carcinogenic PAHs, but heterocyclic PAHs and their alkylated derivatives are also of concern due to their high toxicity to humans and animals.[1−4] Although PAHs can be found in air, water, and soil environments, they often accumulate in soil due to their hydrophobic properties and low volatility.[1,3,5] Thus, it is important to remediate contaminated soils to mitigate public exposure. However, current remediation approaches face significant challenges that underscore the need for innovation. For example, bioremediation (when applicable) is relatively slow and may produce toxic byproducts,[6,7] while several physicochemical approaches are energy-intensive and marginally cost-effective.[8,9]

Pyrolytic treatment is rapidly gaining attention as a fast, reliable, and practical solution to remediate and detoxify PAH-contaminated soils.[10] Because it uses relatively mild temperatures (350−550 °C), pyrolysis can efficiently remove heavy hydrocarbons[8] while retaining soil components necessary for fertility restoration.[10−13] Even though their energy requirements are significantly lower than those of other thermal

Received: May 14, 2024
Revised: July 10, 2024
Accepted: July 11, 2024
Published: July 18, 2024

treatment processes like soil incineration,[8] they remain a significant cost driver and sustainability challenge. Thus, there is growing interest in decreasing the required treatment temperature and associated energy requirements for pyrolytic treatment of contaminated soil through amendments such as hematite or red mud.[14−18] For example, the addition of 5 wt % red mud to petroleum-contaminated soil (prior to pyrolytic treatment at 400 °C for 30 min) increased the removal of the aromatic fraction by over 66%.[15] Recently, we showed that ion-exchanged Fe(III)-bentonite (i.e., Fe-bentonite) can be used as a catalyst to decrease the pyrolysis treatment temperature needed for high PAH removal.[19,20] We saw significantly higher pyrene removal efficiency using Fe-bentonite (93%) than natural bentonite (48%) or unamended contaminated soil (4%) at the unprecedentedly low temperature of 150 °C with only 15 min treatment time.[19]

Density functional theory (DFT) shows that pyrene has stronger adsorption to clays with reducible Fe(III) sites than surfaces with less-reducible cationic transition metals (Cu(II) or Zn(II)),[19] and suggests that PAH pyro-catalytic treatment may be facilitated by direct electron transfer from the π-bonds of PAHs to cationic Fe(III) sites within the bentonite structure.[21] Such electron transfer would destabilize the PAH molecule by forming an aromatic radical, leading to subsequent polymerization and char formation.[12,22−26] This proposed PAH pyrolysis initiation step differs from non-catalytic pyrolysis, which typically involves thermal cracking at temperatures above 350 °C.[12,23,27−33] Accordingly, we postulate that PAHs with lower ionization potential (IP) should degrade more easily at lower pyrolysis temperatures. However, this mechanism has not been experimentally evaluated. Moreover, direct electron transfer will not take place if the PAHs cannot access the Fe(III) sites that serve as reaction centers. Thus, it is important to understand how other PAH properties besides IP, such as PAH hydrophobicity and ring size, affect pyro-catalytic PAH degradation on clay and soil surfaces, and the resulting kinetics.

In this study, we assess the pyro-catalytic degradation of various PAHs (naphthalene, pyrene, benz(a)anthracene, and benzo(g,h,i)perylene) with different ring numbers, IPs, and hydrophobicity (log K_{ow}) in the presence of Fe-bentonite at relatively low pyrolysis temperatures. We combine experimental and DFT methods to determine if (under similar mass transfer limitations) PAHs with lower IP are more easily removed by pyro-catalytic treatment to assess the direct electron transport mechanism. We also assess potential confounding effects from differences in PAH hydrophobicity and number of rings, which may hinder access to catalytic sites. Thus, this study informs rate-limiting mechanisms and pathways for pyro-catalytic remediation of PAH-contaminated soils.

MATERIALS AND METHODS

Materials. Pure bentonite (Sigma-Aldrich) was used to prepare iron ion-exchanged bentonite. Anhydrous iron(III) nitrate (nonahydrate, >98%), Pyrene (98%), Benz(a)-anthracene (99%), and Benzo(g,h,i)perylene (98%) were purchased from Sigma-Aldrich. Naphthalene (≥98%, TCI America) was obtained from Thermo Fisher Scientific. All chemicals were used as received. The background soil (43% clay and 1.57% OM) used in our previous work,[19] collected from Rice University in Houston, TX, was also used for this study. The soil was analyzed for agronomic properties by the Texas A&M Soil, Water, and Forage Testing Laboratory (Table S1). After collection, the soil was dried at 60 °C for 72 h,[19] homogenized, sieved, and stored in closed glass containers before use.

Preparation of Fe-Bentonite. The preparation of the iron ion-exchanged clay was conducted by liquid phase ion-exchange. As in our previous work,[19,20] 20 g of bentonite was added to 400 mL of 0.6 N Fe (III) solution. The mixture was covered and stirred at 300 rpm for 24 h, filtered, dried at 105 °C for 24 h, and sieved (<250 μm). The prepared Fe-bentonite samples were stored at room temperature in capped glass vials. The absence of organic matter and other potential reductants (e.g., sulfides) precluded the transformation of Fe(III) to Fe(II) at room temperature. Fe-bentonite was characterized for metal type and content in our previous work.[19] The predominant oxidation state of Fe-bentonite is Fe(III), and the exchanged iron content in the Fe-bentonite sample was approximately 1.8%wt.

Contaminated Clay and Soil Samples. PAH-contaminated Fe-bentonite was prepared by mixing 1 g of Fe-bentonite clay with 1 mL of a solution containing 0.5 mg/mL of either naphthalene, pyrene, benz(a)anthracene, or benzo(g,h,i)-perylene in HPLC-grade acetone solvent. The clay and PAH mixture was stirred and stored at room temperature until acetone evaporated. After contamination, the initial PAH concentration was determined using an ultrasonic extraction method followed by analysis with High-Performance Liquid Chromatography (HPLC), as detailed below.

The background soil was spiked by a mixture of PAHs using a procedure similar to that described above. Briefly, 5 g of uncontaminated soil was placed in a glass vial and spiked with 2 mL each of 0.5 mg/mL naphthalene, pyrene, benz(a)-anthracene, and benzo(g,h,i)perylene in HPLC-grade acetone. The PAH-soil mixture was capped, shaken for 2 min, and then left to evaporate at room temperature.

Pyrolytic Treatment of Contaminated Clays and Soil. Pyrolysis experiments were conducted using a thermogravimetric analyzer (TGA) (Q500, TA Instruments, New Castle, DE), similar to our past work.[19] Briefly, 200 mg of each PAH-contaminated sample was placed in an alumina pan and pyrolyzed under high-purity nitrogen flowing at 100 mL/min. Initially, the samples were heated at 27 °C for 30 min to ensure there is no sample-to-sample variation of initial conditions before ramping at 50 °C/min to the desired pyrolysis temperature (100 or 150 °C). The pyrolysis temperature was held there for 15 min before cooling to room temperature.

HPLC Analysis of Solvent-Extractable PAHs. An extraction was conducted after each pyrolysis run and three samples from each experiment performed at 100 or 150 °C were analyzed for residual PAH concentration. The PAHs were extracted from the soil and clay matrices using the same extraction method as our previous study.[19] Briefly, 100 mg of sample and 2 mL of acetone were placed in a vial and ultrasonicated in an ultrasonic bath for 30 min, centrifuged, and filtered through a 0.2-μm membrane filter. The extracts were stored in 2 mL HPLC vials. Recoveries of PAHs from Fe-bentonite ranged from 83 to 97%.

The PAHs were quantified before and after treatment using HPLC (Shimadzu, LC20AT) equipped with a C-18 column (Agilent, 4.6 × 250 mm, 5 μm particle size) and a UV−Vis photodiode array detector (Shimadzu, SPD-M20A). The mobile phase consisted of water (0.1% (v/v) formic acid) and acetonitrile (0.1% (v/v) formic acid) with a flow rate of

https://doi.org/10.1021/acs.est.4c04811
Environ. Sci. Technol. 2024, 58, 13521−13528

1.0 mL/min and an injection volume of 10 μL. The gradient elution conditions were presented: 45% acetonitrile increased linearly to 85% in 0−5 min. Afterward, 85% acetonitrile increased linearly to 100% in 5−10 min and kept for 10−15 min. Then, 100% acetonitrile decreased linearly to 45% in 15−20 min to initial conditions. The detector was set to a wavelength of 254 nm. PAH levels were estimated using a standard calibration curve with LOD ranging from ~0.8 to 4.4 mg/kg (Table S2).

Density Functional Theory (DFT) Analysis. We utilized the Fe-bentonite model previously established in our work.[19] To model the bentonite surface, we cleaved a (001) facet from a geometry-optimized Montmorillonite bulk structure, which is the primary component of bentonite (Figure S1).[34] The simulation cell dimensions were set to 20.72 Å × 17.96 Å × 30 Å, resulting in a separation of approximately 20 Å between slab layers. All density functional theory (DFT) calculations were conducted using the Vienna ab initio simulation package (VASP 5.4.4)[35] employing the same methodology and convergence criteria as described in our previous work.[19] Further details are provided in the SI (Text S1).

The adsorption energy (E_{ads}) of the PAH molecule on the bentonite surface was calculated according to eq 1

$$E_{ads} = E_{surf\text{-}molecule} - E_{molecule} - E_{surf} \quad (1)$$

where $E_{surf\text{-}molecule}$ represents the total energy of the bentonite surface with the adsorbed PAH molecule, $E_{molecule}$ represents the energy of an isolated PAH molecule placed in a 25 × 25 × 25 Å^3 simulation cell, and E_{surf} represents the energy of the clean bentonite surface. A more negative energy value indicates a stronger binding interaction between the PAH molecule and the surface.

Statistical Analysis. All pyrolysis experiments were run in triplicates. The statistical significance of differences between treated samples was determined using Student's *t* test (two-tailed, 95% confidence level). A Pearson correlation analysis and analysis of variance (ANOVA) were used to determine whether a significant correlation existed between IP and log K_{ow} values of PAHs and the significance of the effect of IP and log K_{ow} on PAH removal efficiency.

RESULTS AND DISCUSSION

Lower Ionization Potential Enhances PAH Pyrocatalytic Degradation Efficiency at Low Temperatures. We pyrolyzed Fe-bentonite (100 °C for 15 min) that had been thoroughly mixed with equal amounts of either naphthalene, pyrene, benz(a)anthracene, or benzo(g,h,i)perylene. Because the bentonite clay used in this study ($Al_2O_3 \cdot 4SiO_2 \cdot H_2O$) does not contain organic matter (OM) or any other impurities that could sorb PAH and hinder access to the catalytic sites, we expect the PAHs to be distributed in the small Fe-enriched bentonite particles and have direct access to the Fe(III) active sites. Figure 1 shows that PAHs with lower IP values experienced higher removal efficiency. Specifically, naphthalene had the highest IP (8.08 eV) and the lowest removal efficiency (54%). The removal efficiencies for pyrene and benz(a)anthracene that have nearly identical IP (7.5 and 7.47 eV) were similar (63 and 61%, respectively). Finally, benzo(g,h,i)perylene had the lowest IP (7.20 eV) and the highest removal efficiency (78%).

Similar removal rates were observed for pyrene and benz(a)anthracene, which have near-identical IP and the same number of rings but different sorption propensity to non-catalytic soil OM[36,37] (reflected by different log K_{ow} values). This suggests that when access to the catalyst site is facilitated (and not hindered, e.g., by sorption to soil OM), PAH removal efficiency is driven by a direct electron transfer (DET) to the Fe(III) sites. Catalytic cracking of hydrocarbons can occur in the presence of clays and transition metals by creating thermally stable Brønsted and Lewis acids on the solid surface.[38,39] These active sites can interact with the unstable π-bonds of PAHs, destabilizing the PAH molecule and promoting subsequent degradation reactions.[21,40−42] We postulate that Fe-bentonite contains active Fe(III) sites and oxygen functional groups capable of accepting electrons and hydrogen atoms from PAHs and promoting further degradation reactions. However, while this reductionist approach with pure ion-exchanged Fe-bentonite facilitated exploration of the DET mechanism, it is not representative of contaminated soils containing natural OM that tend to exhibit significant PAH sorption and low availability to catalytic degradation, as commonly noted for PAH bioremediation[43−45] (where enzymes serve as catalysts).

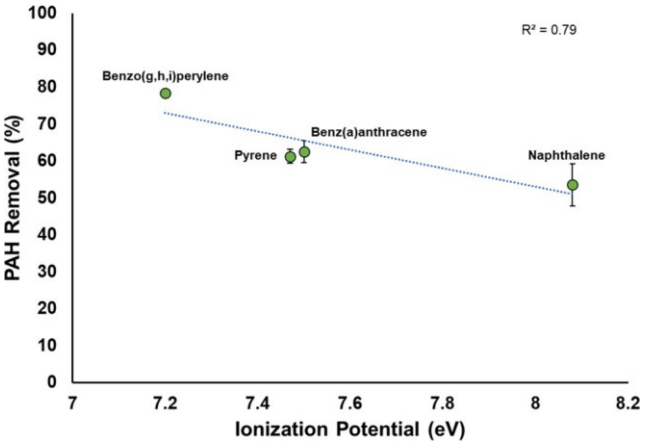

Figure 1. PAHs with lower ionization potential exhibit higher removal efficiency when access to Fe-bentonite active sites is facilitated by mixing. Pyrolytic treatment was conducted at 100 °C for 15 min. Data show the mean ± the standard deviation. PAH removal has a significant negative correlation ($p < 0.05$) with IP.

Lower Ionization Potential Enhances PAH Binding Energy to Fe-bentonite Surfaces. We used DFT to calculate the binding energies of PAHs with varying IP on the Fe-bentonite cation sites as defined by eq 1. To mitigate steric effects caused by larger PAHs, we expanded the surface area by creating a 2 × 2 simulation cell, quadrupling the size of the original bulk surface shown in Figure S1. The enlarged bentonite surface model is illustrated in Figure S2. These calculations enabled us to evaluate the strength of PAH molecule adhesion on the bentonite surface, as well as the extent of charge transfer between the PAH molecules and the surface Fe(III) cations (Figure 2). The computed adsorption energies of PAHs on Fe-bentonite surfaces are as follows: −127 kJ/mol for naphthalene, −176 kJ/mol for pyrene, −189 kJ/mol for benz(a)anthracene, and −205 kJ/mol for benzo(g,h,i)perylene. A lower binding energy indicates stronger binding to the Fe-bentonite surface. The binding energies obtained from DFT calculations align with the experimental trend: PAHs with lower IP bind stronger to the Fe-bentonite surface. Consequently, they are more prone to initiating direct electron transfer from the PAH to the Fe(III) site, thereby

https://doi.org/10.1021/acs.est.4c04811
Environ. Sci. Technol. 2024, 58, 13521−13528

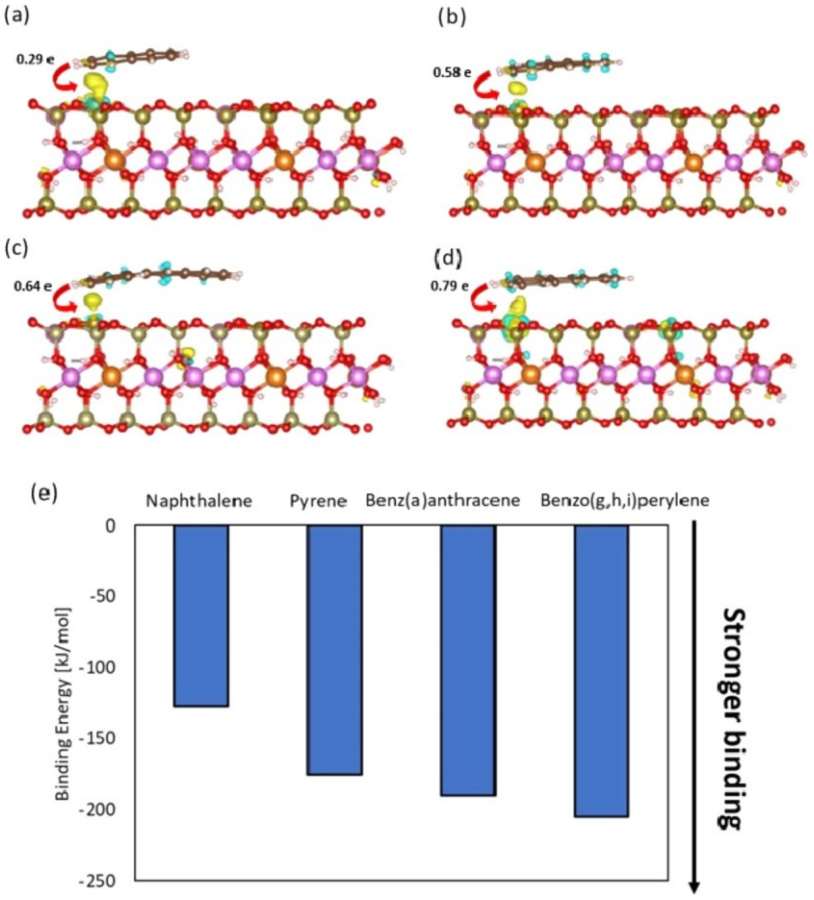

Figure 2. DFT-calculated charge density difference plots for (a) naphthalene (b) pyrene (c) benz(a)anthracene (d) benzo(g,h,i)perylene on the Fe(III)-bentonite surface. Yellow and cyan isosurfaces (0.005 × Å^{-3}) represent electron accumulation and depletion, respectively. (e) PAH adsorption energies on the Fe(III)-bentonite surface.

destabilizing the PAH molecule and promoting pyrolysis. The similar binding strengths of pyrene and benz(a)anthracene on the Fe-bentonite surface aligns with their similar IP values and similar removal efficiencies (Figure 1), which suggests that PAH removal efficiency was primarily driven by DET to Fe(III) sites in Fe-bentonite.

We performed Bader Charge Analysis[47] of the adsorbed PAHs on the Fe(III)-bentonite surface to better understand the extent of charge transfer. The amount of charge transferred was calculated by subtracting the total Bader charge of the isolated PAH molecule in vacuum from the total Bader charge of the PAH molecule when adsorbed on the bentonite surface. The results show that the charge transferred for each molecule during the adsorption process is 0.29 *e* for naphthalene, 0.58 *e* for pyrene, 0.64 *e* for benz(a)anthracene, and 0.79 *e* for benzo(g,h,i)perylene. Greater charge transfer indicates a stronger interaction between the PAH molecule and the Fe(III)-bentonite surface, thus correlating with the stronger binding energies observed for molecules that more readily transfer electron density (i.e., lower IP).

To visualize the charge transfer when PAHs are adsorbed on the Fe-bentonite surface, we subtracted the optimized electron density of the entire adsorbate+surface from that of the isolated surface and adsorbate (Figure 2a−d). The resulting isostructural charge density difference represents the redistribution of charge as PAHs with varying IPs adsorb onto the Fe-bentonite surface. However, it is important to note that the appearance of the isosurfaces is significantly influenced by the shape and size of the molecular orbitals involved in the charge transfer process. Therefore, the visual size of the charge density difference isosurfaces does not quantitatively indicate the amount of charge transferred or the associated change in energy. Nonetheless, we can clearly observe the charge transfer between the PAH molecules and the Fe(III) site on the bentonite surface, indicating the initialization of the DET process during PAH adsorption and followed by subsequent steps of destabilizing the PAH molecules.

Higher PAH Hydrophobicity Decreases Efficiency of Pyro-catalytic Treatment of Contaminated Soil. To explore the possibility of using catalytic amendments to enhance the removal efficiency of a mixture of PAHs from contaminated soil, we first conducted experiments with soil (~1.6% OM content) spiked simultaneously with equal amounts (200 mg/kg) of naphthalene, pyrene, benz(a)-anthracene, and benzo(g,h,i)perylene. Figure 3 shows very little or no removal of pyrene, benz(a)anthracene, and benzo(g,h,i)perylene when the contaminated soil was pyrolyzed at 150 °C for 15 min. No naphthalene was detected in the treated soil, indicating that it did not adsorb strongly to the soil constituents and devolatilized quickly in the initial stages of the TGA experiment (Table 1).

Figure 3 also shows that adding 10 wt % Fe-bentonite to the contaminated soil significantly enhanced PAH removal. Specifically, the removal percentages of pyrene, benz(a)-anthracene, and benzo(g,h,i)perylene increased by 50, 30, and 15%, respectively. These removal percentages are higher

https://doi.org/10.1021/acs.est.4c04811
Environ. Sci. Technol. 2024, 58, 13521−13528

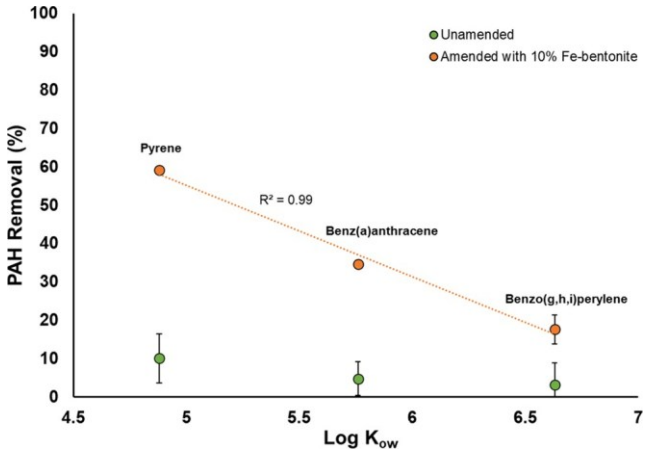

Figure 3. PAH removal in contaminated soil is enhanced by Fe-bentonite amendment (10 wt %), and removal efficiency is hindered by PAH hydrophobicity, which increases sorption tendency. In this PAH-contaminated soil, PAHs with lower log K_{ow} values (Table 1) experienced higher removal at a pyrolysis treatment of 150 °C with a 15 min treatment time. Naphthalene data are not included due to nearly complete removal, mainly associated with volatile losses during thermal treatment.[48] Data show the mean ± the standard deviation. PAH removal in the Fe-bentonite amended system was significantly higher than in the unamended soil control and was negatively correlated ($p < 0.05$) with log K_{ow}.

than those attributable to "dilution" by adding PAH-free Fe-bentonite to the contaminated soil. This agrees with our earlier work showing that amending crude-oil contaminated soil with Fe-bentonite facilitates pyrolysis reactions and decreases the required treatment temperature for hydrocarbon removal.[19,20] Since the Fe-bentonite is the only source of catalytic sites in the amended contaminated soil, Figure 3 suggest that PAHs must first desorb and diffuse into the Fe-bentonite particles to interact with the Fe(III) sites and initiate DET. We recognize there are several sequential mass transfer steps for PAHs to reach catalytic sites: desorption from soil OM or dissolution from oily phase, transport to the surface of bentonite particles, and diffusion into water-filled bentonite pores where most of the Fe(III) sites are located. Any one of these steps can determine the PAH transfer rate and the rate-limiting process may be system- or soil-specific. Although hydrophobicity may enhance PAH diffusion through some organic matrices,[49] PAH hydrophobicity is known to increase the tendency to sorb to soil OM,[50] which would hinder access to inorganic bentonite particles. Noting that the log K_{ow} values follow the order pyrene < benz(a)anthracene < benzo(g,h,i)perylene, Figure 3 shows that less hydrophobic PAHs experienced higher PAH removal efficiency at the low pyrolysis temperature of 150 °C. Pyrene and benz(a)anthracene had statistically different removal efficiencies despite having similar IP and ring numbers but different log K_{ow} values. Benzo(h,*h*,i)perylene had the highest K_{ow} and the lowest removal efficiency. Therefore, PAH access to the catalytic sites is likely limited by sorption to soil. Furthermore, PAH hydrophobicity tends to increase with molecular size, and larger PAH molecules will exhibit slower pore diffusion rates to reach the catalytic sites. Finally, smaller PAHs would desorb easier at temperatures below 200 °C,[51] resulting in higher removal efficiency (Figure 3). While it is difficult to pinpoint the exact reason for the trends of Figure 3, it is clear that PAHs with the lowest hydrophobicity were degraded more efficiently by pyro-catalytic treatment.

Figure 4 shows that IP is inversely correlated with hydrophobicity (log K_{ow}) for the 16 EPA-regulated Priority Pollutants. The data indicate that the IP decreases as the ring number and log K_{ow} of PAHs increase. The stability of PAHs is often determined by their aromaticity, electronic structure, π-bonding interactions, and geometry.[52−56] As PAH size increases, their electrons become less tightly bound, and the

Table 1. Physicochemical Properties of Naphthalene, Pyrene, Benz(a)anthracene, and Benzo(g,h,i)perylene

PAH	Number of Rings	Molecular Weight (g/mol)[a]	Boiling Point (°C)[a]	Ionization Potential (eV)[b]	Log K_{ow}[a]	Chemical Structure
Naphthalene	2	128	218	8.08	3.30	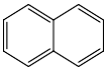
Pyrene	4	202	404	7.50	4.88	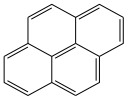
Benz(a)anthracene	4	228	438	7.47	5.76	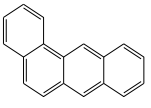
Benzo(g,h,i)perylene	6	276	550	7.20	6.63	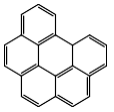

[a]Data from PubChem. [b]Data from NIST Chemistry WebBook.[46]

https://doi.org/10.1021/acs.est.4c04811
Environ. Sci. Technol. 2024, 58, 13521−13528

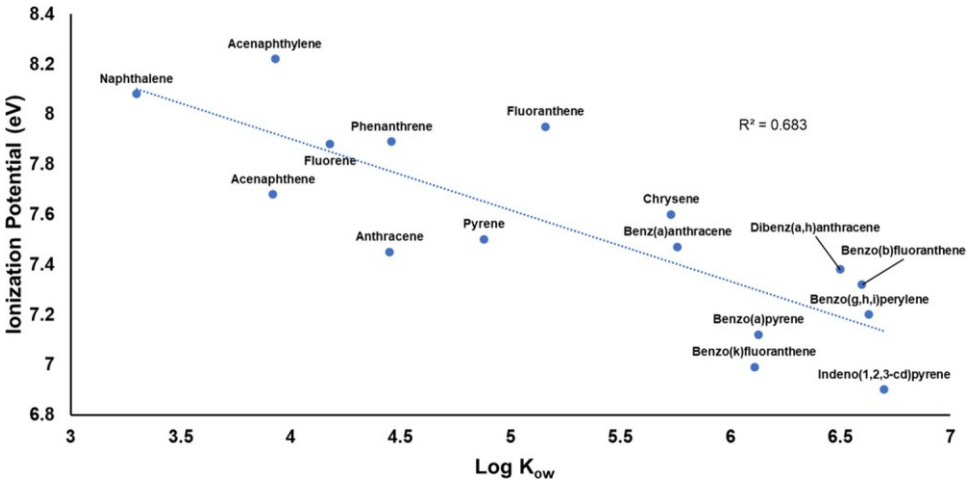

Figure 4. Inverse correlation between IP and log K_{ow} values for EPA's 16 regulated PAHs on the Priority Pollutant List.

electronic structure becomes less stable.[54] The instability is often tied to the HOMO−LUMO energy separation gaps, where larger gaps (commonly associated with smaller compounds) are more stable because adding or removing electrons from these orbitals is unfavorable.[54−57] However, hydrophobicity (log K_{ow}) increases with PAH size, resulting in more prominent hydrophobic interactions.[58] This trend indicates that other factors such as PAH sorption to soil OM and molecular size influencing pore diffusion may limit accessibility to catalytic sites and hinder DET.

ENVIRONMENTAL IMPLICATIONS

If access to the catalyst site is not hindered by sorption (as would be the case for soil with low OM content) and is facilitated by thorough mixing, PAHs with the lowest IP would degrade more efficiently for pyrolytic treatment. This trend, however, may be reversed if the PAHs adsorb strongly on soil constituents like OM because of the inverse correlation between IP and hydrophobicity (Figure 4). This represents an intrinsic trade-off associated with PAH physicochemical properties because, for common soil remediation scenarios, PAHs with higher hydrophobicity will tend to sorb to OM, resulting in hindered access to catalytic sites. Thus, higher hydrophobicity would limit the catalytic benefits of lower IP associated with easier DET to Fe(III) during pyrolytic treatment. Accordingly, soils with high OM and clay content would likely require higher temperatures and treatment duration to remove the more hydrophobic PAHs. Still, adding catalytic amendments to PAH-contaminated soils may significantly enhance PAH removal relative to unamended controls, as shown by the results of Figure 3 (>30% improvement in removal efficiency of pyrene and benz(a)-anthracene by adding 10 wt % Fe-bentonite). This suggests that appropriate catalytic amendments could significantly decrease energy requirements (and associated carbon footprint) to achieve soil cleanup goals, particularly if PAH access to catalytic sites is facilitated by thermal desorption and effective mixing. However, quantification of energy consumption and associated savings would require system-specific techno-economic analyses at later stages to better understand the benefits and limitations of pyro-catalytic soil remediation.

ASSOCIATED CONTENT

Supporting Information

The Supporting Information is available free of charge at https://pubs.acs.org/doi/10.1021/acs.est.4c04811.

Properties of background soil (Table S1); HPLC performance parameters (Table S2); top and side view of DFT bentonite surface model structure (Figure S1); DFT 2 × 2 expanded Fe(III)-bentonite surface (Figure S2); and DFT settings (Text S1) (PDF)

AUTHOR INFORMATION

Corresponding Authors

Thomas P. Senftle − *Department of Chemical and Biomolecular Engineering, Rice University, Houston, Texas 77005, United States;* orcid.org/0000-0002-5889-5009; Email: tsenftle@rice.edu

Pedro J. J. Alvarez − *Department of Civil and Environmental Engineering and Department of Chemical and Biomolecular Engineering, Rice University, Houston, Texas 77005, United States;* orcid.org/0000-0002-6725-7199; Email: alvarez@rice.edu

Authors

Sara B. Denison − *Department of Civil and Environmental Engineering, Rice University, Houston, Texas 77005, United States*

Peixuan Jin − *Department of Chemical and Biomolecular Engineering, Rice University, Houston, Texas 77005, United States*

Kyriacos Zygourakis − *Department of Chemical and Biomolecular Engineering, Rice University, Houston, Texas 77005, United States;* orcid.org/0000-0002-1044-1139

Complete contact information is available at: https://pubs.acs.org/10.1021/acs.est.4c04811

Notes

The authors declare no competing financial interest.

ACKNOWLEDGMENTS

Research reported in this publication was supported by the National Institute of Environmental Health Sciences of the National Institutes of Health [Grant Number P42ES027725]. The content is solely the authors' responsibility and does not

necessarily represent the official views of the National Institutes of Health. PJ and TPS acknowledge partial funding support from the National Science Foundation (Awards # CBET-2143941 and EEC-1449500).

REFERENCES

(1) Agency for Toxic Substances and Disease Registry, Division of Toxicology and Human Health Sciences. Polycyclic Aromatic Hydrocarbons (PAHs) - ToxFAQs, 1996.
(2) Andersson, J. T.; Achten, C. Time to Say Goodbye to the 16 EPA PAHs? Toward an Up-to-Date Use of PACs for Environmental Purposes. *Polycyclic Aromat. Compd.* 2015, *35* (2−4), 330−354.
(3) Gehle, K. Agency for Toxic Substances and Disease Registry (ATSDR) Case Studies in Environmental Medicine Toxicity of Polycyclic Aromatic Hydrocarbons (PAHs), 2009.
(4) Some Non-Heterocyclic Polycyclic Aromatic Hydrocarbons and Some Related Occupational Exposures. In *IARC Monographs on the Evaluation of Carcinogenic Risks to Humans*; IARC Working Group on the Evaluation of Carcinogenic Risks to Humans, International Agency for Research on Cancer, Ed.; IARC Press; Distributed by World Health Organization: Lyon, France: Geneva, 2010.
(5) Hussain, K.; Hoque, R. R.; Balachandran, S.; Medhi, S.; Idris, M. G.; Rahman, M.; Hussain, F. L. Monitoring and Risk Analysis of PAHs in the Environment. In *Handbook of Environmental Materials Management*; Hussain, C. M., Ed.; Springer International Publishing: Cham, 2018; pp 1−35 DOI: 10.1007/978-3-319-58538-3_29-2.
(6) Kuppusamy, S.; Thavamani, P.; Venkateswarlu, K.; Lee, Y. B.; Naidu, R.; Megharaj, M. Remediation Approaches for Polycyclic Aromatic Hydrocarbons (PAHs) Contaminated Soils: Technological Constraints, Emerging Trends and Future Directions. *Chemosphere* 2017, *168*, 944−968.
(7) Chibwe, L.; Geier, M. C.; Nakamura, J.; Tanguay, R. L.; Aitken, M. D.; Simonich, S. L. M. Aerobic Bioremediation of PAH Contaminated Soil Results in Increased Genotoxicity and Developmental Toxicity. *Environ. Sci. Technol.* 2015, *49* (23), 13889−13898.
(8) Vidonish, J. E.; Zygourakis, K.; Masiello, C. A.; Sabadell, G.; Alvarez, P. J. Thermal Treatment of Hydrocarbon-Impacted Soils: A Review of Technology Innovation for Sustainable Remediation. *Engineering* 2016, *2* (4), 426−437.
(9) Exner, J. H. Alternatives to Incineration in Remediation of Soil and Sediments Assessed. *Rem. J.* 1995, *5* (3), 1−18.
(10) Song, W.; Vidonish, J. E.; Kamath, R.; Yu, P. F.; Chu, C.; Moorthy, B.; Gao, B. Y.; Zygourakis, K.; Alvarez, P. J. J. Pilot-Scale Pyrolytic Remediation of Crude-Oil-Contaminated Soil in a Continuously-Fed Reactor: Treatment Intensity Trade-Offs. *Environ. Sci. Technol.* 2019, *53* (4), 2045−2053.
(11) Vidonish, J. E.; Zygourakis, K.; Masiello, C. A.; Gao, X.; Mathieu, J.; Alvarez, P. J. Pyrolytic Treatment and Fertility Enhancement of Soils Contaminated with Heavy Hydrocarbons. *Environ. Sci. Technol.* 2016, *50* (5), 2498−2506.
(12) Vidonish, J. E.; Alvarez, P. J. J.; Zygourakis, K. Pyrolytic Remediation of Oil-Contaminated Soils: Reaction Mechanisms, Soil Changes, and Implications for Treated Soil Fertility. *Ind. Eng. Chem. Res.* 2018, *57* (10), 3489−3500.
(13) Li, J.; Lin, F.; Yu, H.; Tong, X.; Cheng, Z.; Yan, B.; Song, Y.; Chen, G.; Hou, L.; Crittenden, J. C. Biochar-Assisted Catalytic Pyrolysis of Oily Sludge to Attain Harmless Disposal and Residue Utilization for Soil Reclamation. *Environ. Sci. Technol.* 2023, *57* (17), 7063−7073.
(14) Liu, Y. Q.; Zhang, Q.; Wu, B.; Li, X. D.; Ma, F. J.; Li, F. S.; Gu, Q. B. Hematite-Facilitated Pyrolysis: An Innovative Method for Remediating Soils Contaminated with Heavy Hydrocarbons. *J. Hazard. Mater.* 2020, *383*, No. 121165, DOI: 10.1016/j.jhazmat.2019.121165.
(15) Liu, Y.; Li, X.; Zhang, W.; Dou, J.; Zhang, Q.; Ma, F.; Gu, Q. Effect and Mechanisms of Red Mud Catalyst on Pyrolysis Remediation of Heavy Hydrocarbons in Weathered Petroleum-Contaminated Soil. *J. Environ. Chem. Eng.* 2021, *9* (5), No. 106090.
(16) Liu, Y.; Li, X.; Zhang, W.; Ma, F.; Zhang, Q.; Gu, Q. Pyrolysis of Heavy Hydrocarbons in Weathered Petroleum-Contaminated Soil Enhanced with Inexpensive Additives at Low Temperatures. *J. Cleaner Prod.* 2021, *302*, No. 127017.
(17) Oden, C. P.; Werth, C. J.; Notini, L.; Katz, L. E. Fate of Pyrene on Mineral Surfaces during Thermal Remediation as a Function of Temperature. *Environ. Sci.: Processes Impacts* 2022, *24* (8), 1181−1194.
(18) Lin, F.; Yu, H.; Li, J.; Zygourakis, K.; Li, R.; Cheng, Z.; Yan, B.; Chen, G. Investigation on the Interaction between Oil Compositions and Soil Minerals with the Targets of Resource Recovery and Harmless Disposal of Oily Sludges by Pyrolysis. *ACS EST Eng.* 2023, *3* (5), 734−744.
(19) Denison, S. B.; Jin, P.; Dias Da Silva, P.; Chu, C.; Moorthy, B.; Senftle, T. P.; Zygourakis, K.; Alvarez, P. J. J. Pyro-Catalytic Degradation of Pyrene by Bentonite-Supported Transition Metals: Mechanistic Insights and Trade-Offs with Low Pyrolysis Temperature. *Environ. Sci. Technol.* 2023, *57*, 14373−14383.
(20) Denison, S. B.; Da Silva, P. D.; Koester, C. P.; Alvarez, P. J. J.; Zygourakis, K. Clays Play a Catalytic Role in Pyrolytic Treatment of Crude-Oil Contaminated Soils That Is Enhanced by Ion-Exchanged Transition Metals. *J. Hazard. Mater.* 2022, *437*, No. 129295.
(21) Mahadevi, A. S.; Sastry, G. N. Cation−π Interaction: Its Role and Relevance in Chemistry, Biology, and Material Science. *Chem. Rev.* 2013, *113* (3), 2100−2138.
(22) Gao, Y.; Zygourakis, K. Kinetic Study of the Pyrolytic Treatment of Petroleum-Contaminated Soils. *Ind. Eng. Chem. Res.* 2019, *58* (25), 10829−10843.
(23) Savage, P. E.; Klein, M. T.; Kukes, S. G. Asphaltene Reaction Pathways. 1. Thermolysis. *Ind. Eng. Chem. Process Des. Dev.* 1985, *24* (4), 1169−1174.
(24) LaMarca, C.; Libanati, C.; Klein, M. T.; Cronauer, D. C. Enhancing Chain Transfer during Coal Liquefaction: A Model System Analysis. *Energy Fuels* 1993, *7* (4), 473−478.
(25) Gray, M. R.; McCaffrey, W. C. Role of Chain Reactions and Olefin Formation in Cracking, Hydroconversion, and Coking of Petroleum and Bitumen Fractions. *Energy Fuels* 2002, *16* (3), 756−766.
(26) Reyniers, G. C.; Froment, G. F.; Kopinke, F.-D.; Zimmermann, G. Coke Formation in the Thermal Cracking of Hydrocarbons. 4. Modeling of Coke Formation in Naphtha Cracking. *Ind. Eng. Chem. Res.* 1994, *33* (11), 2584−2590.
(27) Berry, A. G. V.; Edgeworth-Johnstone, R. Petroleum Coke. Formation and Properties. *Ind. Eng. Chem. Fundam.* 1944, *36* (12), 1140−1144.
(28) Banerjee, D. K.; Laidler, K. J.; Nandi, B. N.; Patmore, D. J. Kinetic Studies of Coke Formation in Hydrocarbon Fractions of Heavy Crudes. *Fuel* 1986, *65*, 480.
(29) Wiehe, I. A. A Phase-Separation Kinetic Model for Coke Formation. *Ind. Eng. Chem. Res.* 1993, *32* (11), 2447−2454.
(30) Savage, P. E. Mechanisms and Kinetics Models for Hydrocarbon Pyrolysis. *J. Anal. Appl. Pyrolysis* 2000, *54* (1), 109−126.
(31) Yasar, M.; Trauth, D. M.; Klein, M. T. Asphaltene and Resid Pyrolysis. 2. The Effect of Reaction Environment on Pathways and Selectivities. *Energy Fuels* 2001, *15*, 504−509.
(32) Haner, J.; Rankin, K.; Bejan, D.; Bunce, N. J. Industrial Coke as an Electrode Material for Environmental Remediation. *Ind. Eng. Chem. Res.* 2008, *47* (8), 2511−2517.
(33) Appleby, W. G.; Gibson, J. W.; Good, G. M. Coke Formation in Catalytic Cracking. *Ind. Eng. Chem. Proc. Des. Dev.* 1962, *1* (2), 102−110.
(34) Viani, A.; Gualtieri, A. F.; Artioli, G. The Nature of Disorder in Montmorillonite by Simulation of X-Ray Powder Patterns. *Am. Mineral.* 2002, *87* (7), 966−975.
(35) Kresse, G.; Furthmüller, J. Efficiency of Ab-Initio Total Energy Calculations for Metals and Semiconductors Using a Plane-Wave Basis Set. *Comput. Mater. Sci.* 1996, *6* (1), 15−50.

(36) Baker, J. R.; Mihelcic, J. R.; Luehrs, D. C.; Hickey, J. P. Evaluation of Estimation Methods for Organic Carbon Normalized Sorption Coefficients. *Water Environ. Res.* 1997, *69* (2), 136−145.
(37) Schenzel, J.; Goss, K.-U.; Schwarzenbach, R. P.; Bucheli, T. D.; Droge, S. T. J. Experimentally Determined Soil Organic Matter−Water Sorption Coefficients for Different Classes of Natural Toxins and Comparison with Estimated Numbers. *Environ. Sci. Technol.* 2012, *46* (11), 6118−6126.
(38) Hettinger, W. P. Contribution to Catalytic Cracking in the Petroleum Industry. *Appl. Clay Sci.* 1991, *5* (5−6), 445−468.
(39) Fatimah, I.; Fadillah, G.; Yanti, I.; Doong, R. Clay-Supported Metal Oxide Nanoparticles in Catalytic Advanced Oxidation Processes: A Review. *Nanomaterials* 2022, *12* (5), 825.
(40) Jia, H. Z.; Zhao, S.; Shi, Y. F.; Zhu, L. Y.; Wang, C. Y.; Sharma, V. K. Transformation of Polycyclic Aromatic Hydrocarbons and Formation of Environmentally Persistent Free Radicals on Modified Montmorillonite: The Role of Surface Metal Ions and Polycyclic Aromatic Hydrocarbon Molecular Properties. *Environ. Sci. Technol.* 2018, *52* (10), 5725−5733.
(41) Jia, H. Z.; Zhao, J. C.; Li, L.; Li, X. Y.; Wang, C. Y. Transformation of Polycyclic Aromatic Hydrocarbons (PAHs) on Fe(III)-Modified Clay Minerals: Role of Molecular Chemistry and Clay Surface Properties. *Appl. Catal., B* 2014, *154*−*155*, 238−245.
(42) Qu, X. L.; Liu, P.; Zhu, D. Q. Enhanced Sorption of Polycyclic Aromatic Hydrocarbons to Tetra-Alkyl Ammonium Modified Smectites via Cation-Pi Interactions. *Environ. Sci. Technol.* 2008, *42* (4), 1109−1116.
(43) Ukalska-Jaruga, A.; Smreczak, B. The Impact of Organic Matter on Polycyclic Aromatic Hydrocarbon (PAH) Availability and Persistence in Soils. *Molecules* 2020, *25* (11), 2470.
(44) Karaca, G.; Baskaya, H. S.; Tasdemir, Y. Removal of Polycyclic Aromatic Hydrocarbons (PAHs) from Inorganic Clay Mineral: Bentonite. *Environ. Sci. Pollut Res.* 2016, *23* (1), 242−252.
(45) Lu, L.; Zhu, L. Effect of Soil Components on the Surfactant-Enhanced Soil Sorption of PAHs. *J. Soils Sediments* 2012, *12* (2), 161−168.
(46) Talrose, V.; Stern, E. B.; Goncharova, A. A.; Messineva, N. A.; Trusova, N. V.; Efimkina, M. V. IE Value. In *NIST Standard Reference Database Number 69*; Linstrom, P.; Mallard, W. G., Eds.; National Institute of Standards and Technology: Gaithersburg MD, 20899.
(47) Bader, R. F. W. Atoms in Molecules. *Acc. Chem. Res.* 1985, *18* (1), 9−15.
(48) Jia, C.; Batterman, S. A Critical Review of Naphthalene Sources and Exposures Relevant to Indoor and Outdoor Air. *Int. J. Environ. Res. Public Health* 2010, *7* (7), 2903−2939.
(49) Mayer, P.; Fernqvist, M. M.; Christensen, P. S.; Karlson, U.; Trapp, S. Enhanced Diffusion of Polycyclic Aromatic Hydrocarbons in Artificial and Natural Aqueous Solutions. *Environ. Sci. Technol.* 2007, *41* (17), 6148−6155.
(50) Schwarzenbach, R. P.; Imboden, D. M.; Gschwend, P. M. Sorption I: General Introduction and Sorption Processes Involving Organic Matter. *Environ. Org. Chem.* 2002, *2*, 275−330, DOI: 10.1002/0471649643.ch9.
(51) Renoldi, F.; Lietti, L.; Saponaro, S.; Bonomo, L.; Forzatti, P. *Thermal Desorption Of A PAH-Contaminated Soil: A Case Study*, 2003.
(52) Gershoni-Poranne, R.; Rahalkar, A. P.; Stanger, A. The Predictive Power of Aromaticity: Quantitative Correlation between Aromaticity and Ionization Potentials and HOMO−LUMO Gaps in Oligomers of Benzene, Pyrrole, Furan, and Thiophene. *Phys. Chem. Chem. Phys.* 2018, *20* (21), 14808−14817.
(53) Gallegos, E. J. Mass Spectrometry and Ionization Energies of Some Condensed-Ring Aromatic and Heterocyclic Compounds. *J. Phys. Chem. A* 1968, *72* (10), 3452−3456.
(54) Bourgalais, J.; Mercier, X.; Al-Mogren, M. M.; Hochlaf, M. Accurate Prediction of Adiabatic Ionization Energies for PAHs and Substituted Analogues. *J. Phys. Chem. A* 2023, *127* (40), 8447−8458.
(55) Xu, Y.; Chu, Q.; Chen, D.; Fuentes, A. HOMO−LUMO Gaps and Molecular Structures of Polycyclic Aromatic Hydrocarbons in Soot Formation. *Front. Mech. Eng.* 2021, *7*, No. 744001.
(56) Aihara, J.-i. Reduced HOMO−LUMO Gap as an Index of Kinetic Stability for Polycyclic Aromatic Hydrocarbons. *J. Phys. Chem. A* 1999, *103* (37), 7487−7495.
(57) Apriliyanto, Y. B.; Battaglia, S.; Evangelisti, S.; Faginas-Lago, N.; Leininger, T.; Lombardi, A. Toward a Generalized Hückel Rule: The Electronic Structure of Carbon Nanocones. *J. Phys. Chem. A* 2021, *125* (45), 9819−9825.
(58) Honda, M.; Mukai, K.; Nagato, E.; Uno, S.; Oshima, Y. Correlation between Polycyclic Aromatic Hydrocarbons in Wharf Roach (Ligia Spp.) and Environmental Components of the Intertidal and Supralittoral Zone along the Japanese Coast. *Int. J. Environ. Res. Public Health* 2021, *18* (2), 630.